Journal of Assisted Reproduction and Genetics (2022) 39:441–459
https://doi.org/10.1007/s10815-021-02373-0

REPRODUCTIVE PHYSIOLOGY AND DISEASE

Paternal alcohol consumption has intergenerational consequences in male offspring

Maite Yael Cambiasso[1] · Lucila Gotfryd[2] · Marcelo Gabriel Stinson[2] · Sol Birolo[3] · Gabriela Salamone[4] · Marina Romanato[1] · Juan Carlos Calvo[1,3] · Vanina Andrea Fontana[2]

Received: 21 September 2021 / Accepted: 1 December 2021 / Published online: 21 March 2022

Abstract

Purpose Alcoholism is a heterogeneous set of disorders caused by ethanol intake. Harmful effects of paternal consumption on the offspring are poorly explored and not fully understood. We analyzed the effect of paternal alcohol consumption on both their own reproductive capacity and that of their male offspring.

Methods We used a model of ethanol consumption (15% v/v in drinking water) for 12 days in adult CF-1 male mice. DNA integrity and post-translational modifications of histones were assessed in sperm; testicular weight, histology, and DNA fragmentation were analyzed. Treated or untreated male mice were mated with non-treated females to obtain two cell embryos that were cultured for 7 days; morphology and embryonic cell death were evaluated. Males of both groups were mated with non-treated females. Adult male offspring was euthanized, and sperm and testicular parameters determined.

Results Paternal ethanol consumption caused histological and epigenetic changes, as well as damage in DNA integrity in the testicular germline and sperm. These alterations gave rise to deleterious effects on embryonic development and to testicular and spermatic changes in the offspring.

Conclusion This study provides critical information on reproductive disturbances brought about by paternal alcohol consumption and the profound impact these could have on the male progeny. The need to explore the effects of paternal alcohol consumption in detail and warn about the importance of controlling alcohol intake for the well-being of future generations should not be underscored.

Keywords Paternal alcohol consumption · Epigenetic mark · Embryo development · Male offspring · Sperm

Introduction

Sexual reproduction is far more prevalent than asexual reproduction [1] and, perhaps, the evolutionarily most well-preserved function in animals [2, 3]. As such, several processes have developed in both males and females to ensure the success of reproductive events. One of these processes is sperm chromatin condensation [4], the exchange of histones for protamines during spermiogenesis, the final stage of spermatogenesis. Replacing histones with protamines changes the nucleosome-based chromatin structure to a toroidal protamine-based one.

Depending on the species, between 2 and 15% of (the original) histones remain in the fully developed spermatozoon. In mice, particularly, 98% of histones are substituted by protamines [5]. The resulting highly condensed chromatin structure (about 6–8 times more condensed than in somatic cells) ensures transcriptional inactivity and provides mechanical and physical stability to the genetic material [6–8].

Nevertheless, some degree of DNA fragmentation and epigenetic changes are expected in the condensed chromatin. Environmental as well as developmental changes in the histones, protamines, or methylation of DNA CG

✉ Vanina Andrea Fontana
v_fontana@yahoo.com

1 CONICET, Instituto de Biología Y Medicina Experimental (IByME), Buenos Aires, Argentina

2 CONICET, Instituto de Química Biológica de La Facultad de Ciencias Exactas Y Naturales IQUIBICEN, Universidad de Buenos Aires, Buenos Aires, Argentina

3 Departamento de Química Biológica, Facultad de Ciencias Exactas Y Naturales (UBA), Buenos Aires, Argentina

4 Instituto de Medicina Experimental (IMEX), CONICET Academia Nacional de Medicina, Buenos Aires, Argentina

bases could be responsible for altered sperm function in aspects such as motility, acrosome reaction, and chromatin decondensation upon entry into the oocyte or even have effects on the progeny [9, 10]. Sperm epigenetic marks are implicated in post-fertilization zygote functionality and may contribute to embryonic development [11]. Many of the genes related to early embryonic development escape the replacement of histones by protamines, suggesting that these epigenetic marks on human sperm chromatin may be transmitted to the embryo [12]. Epigenetic marks found in sperm include active transcription histone tags (H3K4me2 and H3K4me3) present in promoters of genes required for embryonic development and repressive histone tags (H3K27me3) associated with promoters of genes silenced during gamete formation and in early embryos [13].

Reproductive disruptors such as pesticides or herbicides, or the use of recreational or hard drugs, including alcohol consumption (acute or chronic, mild, or severe), could profoundly affect sperm chromatin epigenetic marks and, thus, have a severe impact on reproduction [10]. Recent literature has shown that alcohol-induced epigenetic changes in DNA could be responsible for transgenerational effects in mice [14]. It is also known that chronic exposure of mice to ethanol affects the methylation of genes in their sperm and that these marks are transmitted to their offspring, generating mental disorders [15].

Our laboratory has presented solid evidence of sperm function alteration in the presence of endosulfan [16] or after subchronic alcohol consumption by male mice, evidenced as changes in chromatin decondensation, hypermotility, acrosome reaction, and altered IVF outcome when spermatozoa from treated mice were used to fertilize oocytes from control female mice [17]. Although the mechanisms involved in the effects of paternal alcohol exposure on embryonic development are not yet known, it is suspected that they could occur at the DNA level.

Herein, we analyzed the effects of paternal alcohol consumption on sperm function, DNA integrity, and epigenetic marks, focusing on early embryonic development and on reproductive parameters of adult male offspring. We provide evidence on how alcohol consumption by male mice could not only affect their own sperm physiology but also negatively impact their progeny from the very beginning of embryonic development.

These findings point to the need to continue studying the effects of male alcohol consumption on their offspring, addressing it as a serious and important problem within society considering its possible implications as a serious and important problem within society. Of particular importance is that the detrimental effect of alcohol intake does not impact exclusively on the gametes of the father but can also be found in the progeny and could thus be a matter of consideration in fertility clinics when offering assisted reproductive technologies to infertile couples.

Materials and methods

Animals

Outbred CF-1 sexually mature male and female mice (Mus musculus, CrlFcen:CF1, Mouse Genome Informatic (MGI)) were obtained from the animal facility of the FCEN (Faculty of Exact and Natural Sciences) of the University of Buenos Aires (Buenos Aires, Argentina). They were housed by sex in groups of three mice per cage and maintained at 22 °C with a 12:12-h light/dark cycle. All mice were fed commercial mouse chow (Alimento "Balanceado Cooperación Rata-Ratón" from the Asociación Cooperativa de Alimentos S.A. Buenos Aires, Argentina) and had access to tap water ad libitum.

Alcohol administration and blood alcohol concentration (BAC) assessment

Adult CF-1 male mice, 60 days old on average, and with an approximate body weight of 30 g, were given access to 15% (v/v) ethanol in drinking water for 12 days (treated males), a period long enough to include spermiogenesis [18], while control males received ethanol-free drinking water ad libitum. Control and treated males were weighed at the beginning and at the end of ethanol treatment. Every morning, the drinking volume and the quantity of food consumed were recorded ($n = 10$ mice per experimental group) to monitor the daily liquid, food, and calorie intake (estimated by caloric value of the diet used 3976 kcal/kg). On day 12 of treatment, CF-1 males were killed by cervical dislocation and trunk blood was collected into BD Microtainer® tubes ($n = 5$ mice per experimental group). Blood samples were held at 4 °C for ethanol measurement using a commercial kit (NAD/NADH enzymatic assay, sensitivity 10.1 mg/dL), within 3 h of collection.

Animal experimental procedures were performed in strict accordance with the Guide for Care and Use of Laboratory Animals approved by the National Institutes of Health, reviewed and approved by the CICUAL (Comisión Institucional de Cuidado y Uso de Animales de Laboratorio) of FCEN-UBA (Protocol Number 56/2016). A total of 40 animals were housed in groups of 4 per cage; 20 males were randomly allocated to each group (control $n = 20$; treated $n = 20$), and the number of animals used for each experiment is described in legends.

Epididymal sperm preparation and analysis of sperm parameters

Following treatment with ethanol, male mice were euthanized by cervical dislocation, the epididymides dissected, and both *caudae* removed and transferred into a dish containing 400 µL of in vitro fertilization medium (IVFM: 99.3 mmol/L NaCl, 2.70 mmol/L KCl, 0.50 mmol/L $MgSO_4$ $0.6H_2O$, 1 mg/mL glucose, 0.31 mmol/L $Na_2HPO_4.2H_2O$, 1.80 mmol/L $CaCl_2.H_2O$) [19]. The pH of the medium was adjusted to 7.3 with 25 mmol/L NaOH, and 5.5 µg sodium pyruvate and 0.35 mL L-Na-lactate (60% syrup) were added to a final volume of 100 mL. To recover sperm cells, small incisions were performed in both *caudae*, allowing motile cells to be released over a period of 10 min at 37 °C (swim-out procedure). The sperm suspension was homogenized, and an aliquot collected to determine sperm concentration using a Neubauer chamber, cauda epididymal sperm motility (progressive + nonprogressive sperm), was assessed under phase contrast microscopy in an Olympus CH2 microscope at 400 × magnification.

Analysis of sperm reactive oxygen species (ROS)

Analysis of intracellular ROS generation was performed by flow cytometry. Sperm viability was determined with 5% eosin staining (William Pollack test). Briefly, sperm cells at a final density of 1×10^6 spermatozoa/tube were stained with 5 µM CellROX Green Reagent (Life Technologies Alfagene, Carcavelos, Portugal) for 30 min at 37 °C. Data were recorded as individual cell events using a FACSCanto II TM cytometer (BD Bioscience) and analyzed using the FlowJo v10 software (FlowJo LLC, Ashland, OR). Forward scatter (FSC) and side scatter (SSC) fluorescence data were collected from 10,000 events per sample. Threshold levels for FSC-A and SSC-A were set to exclude signals from cellular debris or morphologically abnormal cells in all samples.

Autofluorescence intensity was determined in each sample (control or treated) prior to the addition of the fluorescent probe to calculate relative fluorescence intensity.

DNA fragmentation (TUNEL) assay in the testicular cell population

DNA fragmentation was analyzed via TUNEL assay (terminal deoxynucleotidyl transferase (TdT)-mediated dUTP nick end-labeling assay) using the in situ cell death detection kit (Roche), according to the manufacturer's instructions. Testes were fixed in 4% paraformaldehyde (PFA) solution for 36 h, embedded in paraffin, and sectioned at 5-µm thickness. Paraffin was removed from testicular sections, and tissues rehydrated.

Afterwards, cross-sections were incubated with proteinase K (20 µg/mL in 10 mM Tris/HCl, pH 7.4) for 20 min at room temperature. Slides were washed with PBS (two times, 5 min each) and then incubated in TUNEL solution (Roche) for 1 h at 37 °C. One extra cross-section was incubated with DNase (1500 IU/mL; Sigma) for 10 min at 37 °C as a positive control, and in another section, TUNEL enzyme solution was omitted as a negative control. Finally, all samples were washed with PBS (two times, 5 min each) and incubated with DAPI for 5 min. Slides were mounted with VECTASHIELD H-1000 medium (Vector Laboratories). Cells from a total of 4 seminiferous tubules per animal were analyzed using an inverted Olympus IX83 microscope, with a Plan-APO N 60 × objective/1,42 oil, excitation/emission filters 368–415 nm/515–530 nm, and 460–495 nm/510–550 nm.

Testis weight and histology

Male mice were euthanized by cervical dislocation to examine testis weight and testicular histology. Testes were fixed in Bouin solution for 24 h, embedded in paraffin, and sectioned at 5-µm thickness. Testicular sections were dewaxed by immersing the slides in fresh xylene twice for 10 min. Slides were then rehydrated with a graded ethanol series, starting with 100%, 100% for 10 min each, followed by 95%, 95%, and 70% for 5 min each, and ending with a 3-min PBS wash. Slides were then stained with Hematoxylin and Eosin using standardized protocols. Stained sections were examined using an Eclipse Ti microscope (Nikon Instruments Inc., Tokyo, Japan). In each experimental group, histology slides were examined for signs of testicular damage. Five randomly selected fields were observed at 100 × and scored on each slide. At least 50 tubules from each male were evaluated.

Testicular cross-sections analyzed were not next to each other to avoid repeatedly counting the same tubule.

Sperm production

The daily sperm production (DSP) in the testis was measured as a parameter of testicular function, following the protocol established by Kyjovska et al. [20], with modifications. This technique relies on the fact that the highly compacted nuclei of elongated spermatids (from stages 14–16) are resistant to homogenization.

One testis per male was dissected and stored at − 70° C until use. The tunica albuginea was removed and discarded, and the remaining tissue weighed and homogenized in 1 ml of 0.05% Triton X-100 solution in PBS for 3 min at 9700 g. Samples were incubated for 30 min on ice.

Subsequently, a 200-µl aliquot of the homogenate was incubated with 200 µl of a 0.08% Trypan Blue solution in

PBS for 5 min. The number of stained elongated spermatid heads was counted in duplicate in a Neubauer hemocytometer under light microscopy at 400× magnification, and the number of spermatids per testis was determined by multiplying the number of cells counted by the dilution factor. The DSP was calculated as the total number of elongated spermatids per testis divided by 4.84, which is the number of days employed by spermatids to develop through stages 14–16 of spermatogenesis. The efficiency (DSP per gram of testis) was calculated as the ratio between DSP and testis weight [21].

In vitro decondensation of sperm chromatin

Each sperm suspension ($8–10 \times 10^6$ spermatozoa/mL) was resuspended in IVFM medium supplemented with 0.3% bovine serum albumin (BSA) and incubated for 90 min at 37 °C in an atmosphere of 5% CO_2 to promote sperm capacitation. After capacitation, sperm nuclear decondensation was induced in vitro in the presence of 10 mmol/L glutathione (GSH) plus 4.6 µmol/L heparin (Hep, 13,500 kDa, 170 IU/mg) for 15, 30, and 60 min. Controls consisted of parallel incubations with GSH or Hep alone (data not shown). After each time, a 30-µL aliquot of the sperm suspension was removed and fixed with an equal volume of 2.5% glutaraldehyde in phosphate-buffered saline (PBS). The percentage of decondensed spermatozoa was determined under phase contrast in a Nikon Eclipse E200 microscope at 400× magnification.

Spermatozoa were classified as unchanged (U), moderately decondensed (M), or grossly decondensed (G) [22]. At least 200 cells were evaluated in each sample. Total sperm decondensation was calculated as the sum of % M and % G (% M + G).

Immunofluorescence analysis of post-translational modifications (PTM) of histones in sperm

Each sperm suspension was incubated for 10 min or less (depending on the degree of decondensation observed) under decondensing conditions (10 mmol/L GSH plus 4.6 µmol/L Hep). A 5-µL aliquot of the sperm suspension was placed into each well of a multiwell plate (4 mm diameter) and allowed to stand for 8 min.

Each well was washed once with PBS, and, after drying, cells were fixed in 4% PFA for 20 min. Cells were then washed with PBS (three times, 10 min each), permeabilized with 0.5% Triton X-100 (Sigma-Aldrich) in PBS and incubated for 30 min at room temperature in a blocking solution (4% BSA in PBS with 0.1% Tween 20). The following primary antibodies were used to detect histone PTMs: anti-H3K4me2 (Cell Signaling, c64g9 (9725), Monoclonal, IgG, Rabbit); anti-H3K27me3 (Cell Signaling, c36b11(9733), Monoclonal, IgG, Rabbit); anti-H3K9me2/me3 (Cell Signaling, 6f12 (5327), Monoclonal, IgG, Mouse); anti-H3K4me3 (Cell Signaling, c42d8 (9751), Monoclonal, IgG, Rabbit); anti-H3K9me (Abcam, ab9045, Polyclonal, IgG, Rabbit); and anti-H4K12ac (Abcam, ab46983, Polyclonal, IgG, Rabbit).

After overnight incubation with primary antibodies, samples were washed with PBS (three times, 10 min each) and incubated with the appropriate secondary antibody (IgG anti-Rabbit-FITC (Sigma, F0382) or IgG anti-Mouse-FITC (Sigma, F0257)) at room temperature for 90 min. Negative controls consisted of omission of the primary antibody. Primary antibodies were used at a dilution of 1:100, and secondary antibodies were used at a dilution of 1:200. Nuclei were stained with DAPI, and slides were mounted with VECTASHIELD (Vector Laboratories, Burlingame, CA). Cells were observed under an inverted Olympus IX83 microscope, using a PlanAPO N 60×/1,42 oil objective, and excitation/emission filters 368–415 nm/515–530 nm and 560–495 nm/510–550 nm. At least 100 cells were evaluated in each category.

Mouse mating and breeding, embryo recovery, collection and culture

Alcohol consumption of treated males was suspended on day 12. Subsequently, treated ($n = 20$) and control ($n = 20$) male mice were mated with non-treated females (60 days old, average body weight of 20 g). Twenty-four hours later, females were inspected for the presence of a vaginal plug. The ratio of females with vaginal plugs to total females was determined to evaluate mating efficiency in control and treated groups. Females with positive vaginal plugs were identified and euthanized by cervical dislocation ($n = 12$ per group) at day 2 of gestation (day 1 = vaginal plug). Two-cell stage embryos were collected from the oviducts and washed with pre-warmed PBS and kept at 37 °C in an atmosphere of 5% CO_2 until seeding. Embryos were counted, and the ratio of one or two-cell embryos to total embryos was determined. Two-cell embryos were cultured for 72 h in 20-µL drops of pre-equilibrated Global Total medium (Life Global Group).

At that point, the number of blastocysts was registered, and culture continued for an additional 96 h in Global Total medium supplemented with 15% (v/v) fetal bovine serum (FBS, Gibco). Cultures were kept at 37 °C in 5% CO_2 in air throughout.

Eight females with vaginal plug from each group were assigned to breeding. Four females were housed per cage for the first 17 days of pregnancy and then isolated until parturition. They received standard mouse chow and tap water ad libitum, were ethanol (EtOH) naïve, and did not have access to EtOH. No differences were found in the length of the gestational period between both groups (data not shown).

Litters with less than 7 individuals were discarded as well as those in which mother cannibalism was observed. We obtained 6 litters from each group; the number of pups and sex distribution was registered after birth. Efforts were made to balance the litter size within a range of 9–10 pups per dam on postnatal day (PD) 2. Offspring were weaned at PD 21 and caged according to sex. On PD 100, male offspring were euthanized, testes weight, and morphology were assessed, and sperm parameters analyzed.

Morphology and surface area of outgrowing blastocysts

Embryo differentiation, growth, and morphology were evaluated in vitro at the post-implantation phase. At the end of the culture period (7 days), two cell embryos could develop from both control and treated groups. Embryos were photographed, and inner cell mass (ICM) and trophoblasts (TB) of each outgrowth were graded according to a previously developed morphological classification [23]. At this stage, the outgrowing embryo consists of a monolayer of spreading TB cells surrounding a protruding aggregate of ICM, and its morphology reflects the capacity of peri-implantation blastocysts to implant in utero [24]. ICM and TB from each outgrowing embryo were characterized as type A or B. It was made according to the following characteristics: type A TB, regular monolayer of cells with a predominantly large elongated epithelioid phenotype corresponding to a giant cell transformation; the outline of the TB outgrowth showing regions with irregular edges; type B TB, irregular or limited monolayer with few giant cells; predominance of regions with smooth edges in the outline of the TB, reflecting limited structural signals of the spreading stages; type A ICM, protruding aggregate of compact cells inside a TB outgrowth; and type B ICM, few, disaggregated, and non-compacted ICM cells inside a TB outgrowth. TB outgrowths without ICM were also observed. Embryos with a hybrid phenotype were frequently observed: type A ICM cells and type B TB cells, or vice versa. Finally, expansion of the embryos' outgrowth was evaluated by calculating their surface area using the Scion ImageJ software 1.53 (National Institutes of Health, Bethesda, MD, USA).

Determination of embryonic cell death

Annexin-V binding to embryonic cells was performed using a commercial kit (Immunotech, Marseille, France). Two-cell embryos from control or treated groups ($n = 3$ males per group, 1 or 2 embryos from each) were cultured for 7 days. Adhered outgrowth embryos were washed with PBS and labelled with annexin-V FITC and DAPI for 20 min at 4 °C and analyzed by two-color fluorescence microscopy in a Nikon Eclipse Ti-E inverted microscope [25]. Pictures were analyzed with ImageJ to assess mean fluorescence intensity. Three fields (~200 pixels each) corresponding to ICM and three to TB were selected from each embryo and fluorescence intensity evaluated in all of them. An average fluorescence intensity for TB and for ICM was obtained for each embryo.

Statistical analyses

Analyses were performed using GraphPad Prism 7.0 (GraphPad Software, San Diego, CA, USA) and data expressed as mean ± standard error of the mean (SEM). Significance level was set to 5% ($\alpha = 0.05$). All datasets were first tested for normal and lognormal distribution using the Kolmogorov–Smirnov test. Those with a lognormal distribution were submitted to a lognormal transformation before statistical analysis.

Differences between control and treated groups were assessed using either an unpaired Student's *t* tests for parametric data or Mann–Whitney *U* tests for non-parametric data, except for the comparison of sex distribution, and number of one or two cell embryos, which were analyzed using two-way analyses of variance (ANOVA).

Differences in testis morphometry and TUNEL assay were assessed using a nested *T* test, also called nested two-way ANOVA or hierarchical ANOVA. Briefly, it fits a mixed effects model with the main factor (in our case, treatment) as a fixed factor and the nested factor (litter or individual) as a random factor.

Results

Alcohol administration and blood alcohol concentration (BAC) assessment

CF1 males from the treated group consumed significantly lower quantities of food ($p = 0.0025$) and liquid ($p < 0.0001$) than control males (Table 1). However, the total calorie intake was similar for both groups. Treated males consumed 7.4 g/kg/day of ethanol with a 16.1% EDC (percentage of ethanol-derived calories) (Table 1).

Treated and control males showed no differences in body weight either at the beginning or at the end of ethanol treatment. Blood alcohol concentration (BAC) was 15–23 mg/dL in treated males, and no alcohol was detected in the blood of control males ($n = 5$ males per group).

Analysis of sperm parameters

Sperm motility and sperm count were routinely assessed prior to the beginning of each experiment, and animals were randomly distributed for the different experiments. We did

Table 1 Evaluation of mice weight and calories intake in control and treated group

	Control	Treated
Food intake (g/kg/day)	181.4 ± 16.8	120.0 ± 4.5**
Liquid intake (g/kg/day)	182.7 ± 9.7	104.9 ± 4.8****
Food calories (kcal/kg/day)	721.2 ± 66.9	477.2 ± 17.9**
Liquid calories (kcal/kg/day)	–	105.5 ± 6.4
Total calories (kcal/kg/day)	721.2 ± 66.9	657.1 ± 60.52
Ethanol intake (g/kg/day)	–	7.4 ± 0.9
% EDC	–	16.1
Initial body weight (g)	40.3 ± 0.9	40.1 ± 0.8
Final body weight (g)	42.6 ± 0.7	40.4 ± 0.8

** $p < 0.01$

**** $p < 0.0001$

Daily food and liquid intake (g or mL/kg/day) and body weight (g) were measured during 12 days of 15% ethanol administration, in both control and treated males. Total calories were calculated from food and ethanol consumption (kcal/kg/day). Mean ethanol intake is expressed in g/kg/day and % EDC (percentage of ethanol-derived calories). Values are expressed as mean ± s.e.m. Student's *t* test, 10 males per group

not find differences in sperm motility between experimental groups (neither in parents nor in F1) (Table 2).

Analysis of sperm reactive oxygen species (ROS)

To study if male ethanol consumption alters the levels of sperm ROS, we analyzed their presence in sperm from both groups. First, we analyzed the sperm viability, and no significant differences were observed between both experimental groups (57 ± 6 in control mice vs. 59 ± 4 in treated mice, mean ± SEM, Student's *t* test, $p > 0.05$, $n = 5$ males per group). Then, sperm were loaded with the CellROX Green Reagent probe and analyzed by flow cytometry (Fig. 1a). The percentage of spermatozoa that presented a positive mark for the fluorogenic probe used was the same in both groups (Fig. 1b). However, the fluorescence intensity was significantly higher ($p = 0.008$) in spermatozoa from treated males than control males (Fig. 1c and d).

DNA fragmentation (TUNEL) assay in the testicular cell population

To assess whether alcohol consumption alters DNA integrity in the germ cell line, we analyzed the incidence of nuclear DNA strand breaks via the TUNEL method. We observed a significant increase in DNA fragmentation in the germline in seminiferous tubules from testes of adult treated mice ($p = 0.036$) (Fig. 1e and f).

Testis weight and histological analysis

We analyzed the weight and morphometric characteristics of the testes to evaluate the effects of alcohol consumption. Testes' weights and the ratio testis weight to body weight of control and treated males were similar (Table 2). In histological sections of testes in the control group, we observed uniformly sized seminiferous tubules, lined by several layers of orderly germinal cells, composed of spermatogonia and Sertoli cells and spermatogenic cells in advanced stages. We observed small lumens with spermatozoa inside, little interstitial space with normal interstitial cells (Leydig cells). Testes of mice in the treated group exhibited histopathological changes in the seminiferous tubules: disorder of germinal cell arrangement, large lumen showing immature germ cells inside and irregular spaces in the epithelium, probably due to the desquamation of spermatogenic cells. We also observed marked expansion of the interstitial space between seminiferous tubules (Fig. 2a).

We determined the diameter of the seminiferous tubules, and no differences were observed between the two groups (Fig. 2b); however, there was a significant increase in the

Table 2 Sperm parameters and testis weight in control and treated mice (parents and F1)

	Father		Offspring	
	Control	Treated	F1 control	F1 treated
Motile sperm (%)	60.11 ± 1.57	64.77 ± 1.29	55.92 ± 1.35	55.70 ± 1.03
Sperm count (10^6/mL)	36.69 ± 2.05	34.61 ± 2.17	36.50 ± 3.49	37.00 ± 3.83
Testis weight (g)	0.113 ± 0.005	0.110 ± 0.006	0.118 ± 0.006	0.099 ± 0.004*
Testis/body weight ($\times 10^3$)	2.58 ± 0.18	2.70 ± 0.14	2.98 ± 0.14	2.41 ± 0.10**

* $p < 0.05$

** $p < 0.01$

The mice of each experimental group were weighed to determine the body weight. Both testes were weighed, and the values were averaged. Testis weight and body weight-relative to testes weights in animals of the F1-treated group were significantly lower than in those of the F1-control group. No significant differences were observed in the other parameters. Results are expressed as mean ± SEM, Student's *t* test, $n = 11$ males per group

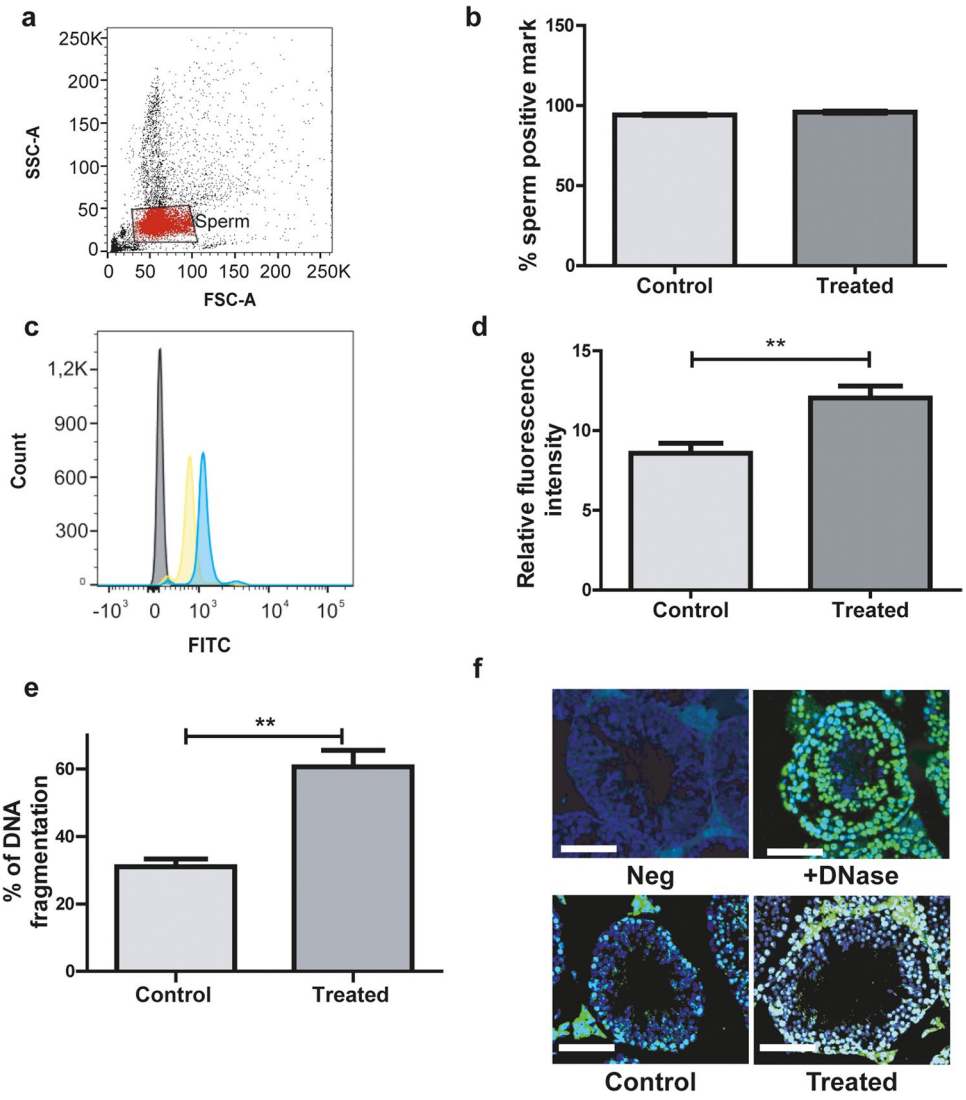

Fig. 1 Analysis of ROS in sperm samples from control and treated males. **a** FSC and SSC fluorescence data were collected from 10,000 events per sample. Threshold levels for FSC-A and SSC-A were set to exclude signals from cellular debris or abnormal morphology for all samples. **b** Percentage of spermatozoa evidencing the presence of ROS. **c** Representative histogram of the fluorescence spectra obtained through flow cytometry for sperm samples in absence of reporter probe (grey), and sperm samples corresponding to control (yellow) or treated (blue) mice. **d** Sperm relative fluorescence intensity (positive mark for ROS relative to negative control sample). (**b**, **d**) $n=5$ males per group, $^{**}p<0.01$, Student's t test. **e** TUNEL assay results expressed as percentage of DNA fragmentation, $n=6$ males per group with a minimum of 4 randomly selected fields per testis. **f** Representative merge on immunofluorescence images of the TUNEL assay (green: positive TUNEL; blue: DAPI). Scale bar, 100 µm. Nested t test. $^{**}p<0.01$

size of the lumen of the seminiferous tubules in the treated group ($p=0.026$) (Fig. 2c). No differences were found in the thickness of the epithelium of the seminiferous tubules (Fig. 2d). The organization of the tubules was not altered in treated mice, but Fig. 2a clearly shows the increase in the size of the lumen of the seminiferous tubules, as well as an apparent decrease in the amount of sperm inside them. Considering these observations, we analyzed the daily sperm production. The treated group showed a statistically significant decrease in the DSP ($p=0.0132$) and in the efficiency of DSP (DSP per gram of testis) ($p=0.0060$) in comparison with the control group (Fig. 2a and f, respectively).

Immunofluorescence analysis of post-translational modifications (PTM) of histones in sperm

To investigate whether male alcohol consumption alters the levels of modified histones in mouse sperm chromatin, we determined their presence by immunofluorescence in cauda epididymal sperm. Since histone modifications cannot be visualized by direct immunostaining because they are few and masked by the compacted chromatin, the sperm had to be previously decondensed.

Mouse spermatozoa were positive for all histone modifications studied (H3K4me3, H3K27me3, H3K9me2/me3, H3K4me2, H3K9me, H4K12ac). Male alcohol consumption significantly decreased sperm histone epigenetic mark H3K4me3 in the treated group ($p=0.032$) (Fig. 3a), whereas no differences were observed for the following epigenetic marks: H3K27me3, H3K9me2/me3, H3K4me2, H3K9me, and H4K12ac (Fig. 3b-f). The general localization of the modified histones was shared by both experimental groups, with each histone PTM having a specific localization within the spermatozoon. The positive H3K4me3 mark in the sperm head was observed in the apical region. The positive H3K27me3 mark was localized in the inner region of

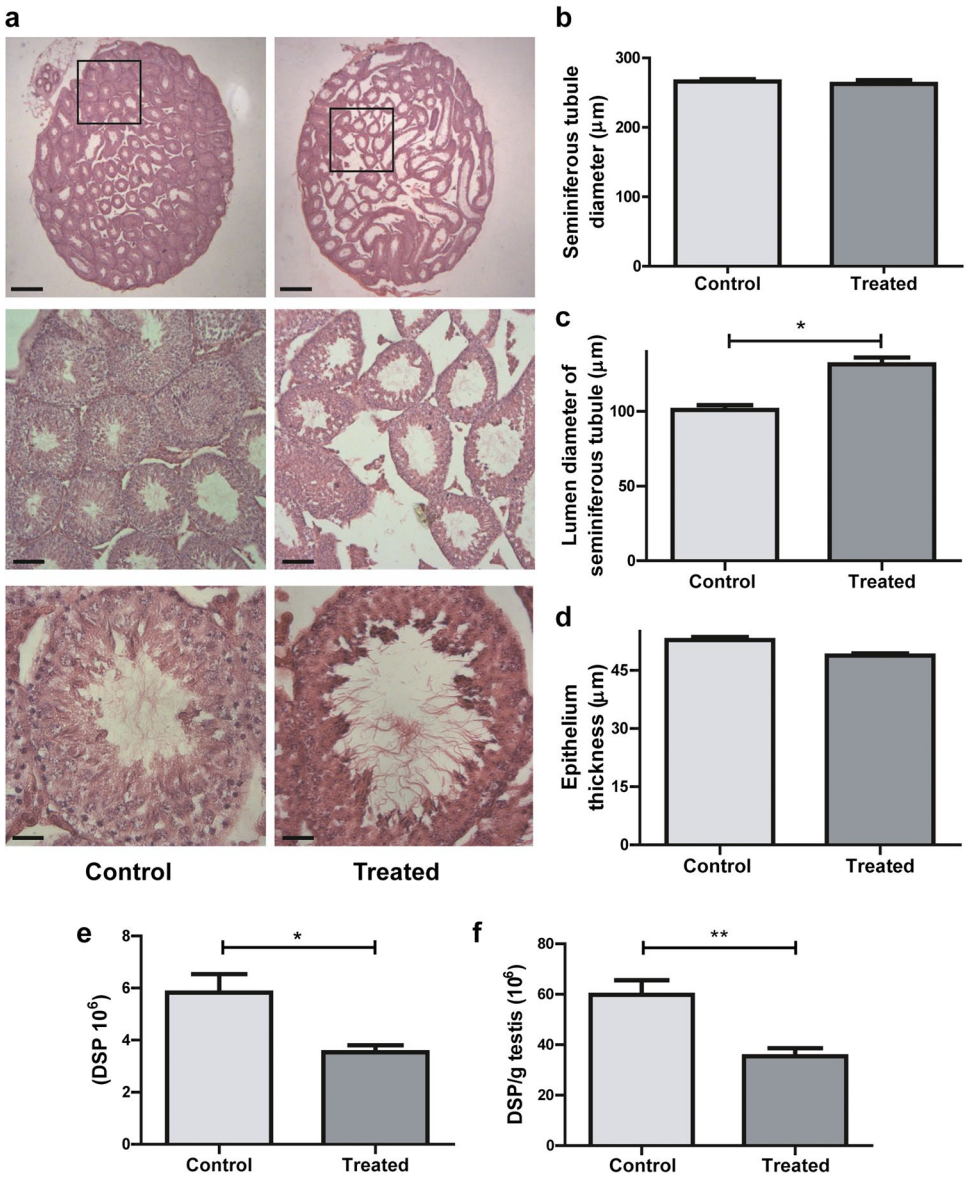

Fig. 2 Testicular histology. **a** Cross-section images representative of testicular morphology in control (left panel) and treated (right panel) groups. Stained with Hematoxylin and Eosin. Original magnification of images: 20 × up, 100 × middle, 400 × down (scale bar: 500 µm, 100 µm and 25 µm, respectively). **b**–**d** Morphometric analysis of the testes: diameters of seminiferous tubules (**b**), their lumens (**c**), and the thickness of the seminiferous tubule epithelium (**d**). At least 50 tubules were evaluated for each male. $n = 6$ males per group with a minimum of 4 randomly selected fields per testis. Nested t test. $^{*}p < 0.05$. Dates were transformed using the lognormal formula to assume normal distribution. **e** Daily sperm production per testis (DSP) and **f** efficiency (DSP per gram of testis) of sperm production in control and treated group, $n = 5$ males per group. Student's t test $^{*}p < 0.05$, $^{**}p < 0.01$

the sperm heads. H3K9me2/me3 marks were distributed throughout the head, presenting a greater intensity in the inner region. Positive marks for H3K4me2 were distributed homogeneously across the head. H3K9me was localized in the posterior and basal regions of the sperm head. H4K12ac presented an intense mark in the apical region of the sperm head (Fig. 3g).

In vivo *functional evaluation of sperm from treated males*

We analyzed the number of positive vaginal plugs after mating with control or treated males (Fig. 4a) and did not find significant differences between groups ($p > 0.05$). Additionally, after 24 h of detecting a positive vaginal plug, we registered the number of one (oocyte and/or zygote) or two-cell embryos per female. No differences were detected between groups in either measurement (Fig. 4b).

We further evaluated the effect of paternal alcohol consumption on early embryo development. Two-cell embryos from females mated with control or treated males were cultured for 7 days. At day 3 of culture, we evaluated the proportion of two cell embryos that reached the blastocyst stage and did not observe any difference between both groups (Fig. 4c). When we measured the area of trophoblast outgrowth at day 7 of culture, there were no significant differences between groups (Fig. 4d). Nonetheless, we did notice an alteration in embryonic development and cell differentiation, evidenced by changes in embryo morphology. As previously described, outgrowing embryos obtained from each fecundated female were classified according to ICM and TB morphologies into types A (Fig. 4ea´) and B

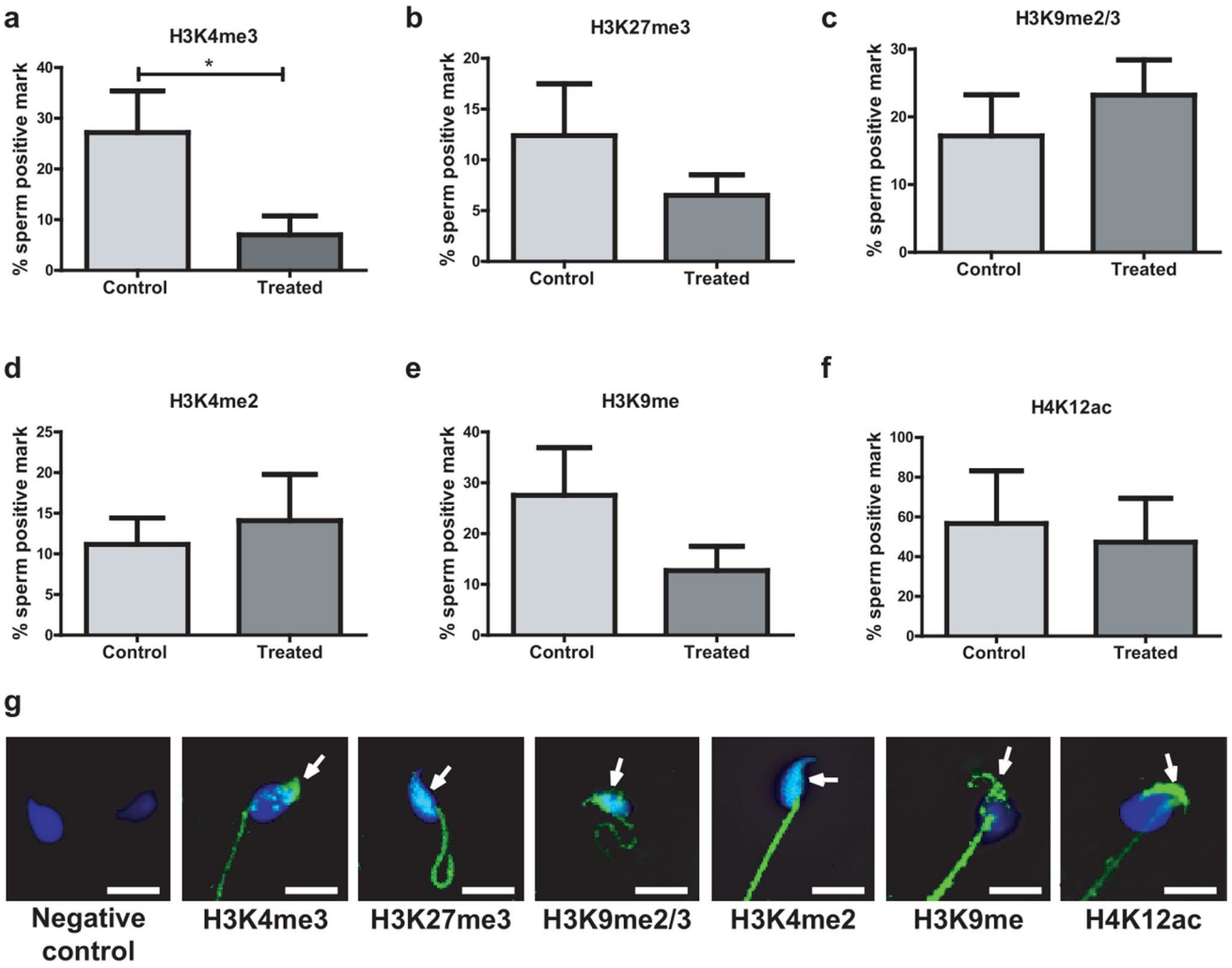

Fig. 3 Post-translational modifications (PTM) of histones in spermatozoa of control or treated mice. **a** H3K4me3, **b** H3K27me3, **c** H3K9me2/3, **d** H3K4me2, **e** H3K9me, **f** H4K12ac. **g** Representative images of the localization of the positive marks (green) of PTM of histones in sperm of control and treated mice. The sperm nucleus is labeled with DAPI (blue). Scale bar, 10 µm. Data were analyzed with Student's *t* test for parametric data or Mann–Whitney *U* tests for non-parametric data. $*p < 0.05$. $n = 10$ males per group. The arrows indicate the positive mark inside the sperm

(Fig. 4eb´, c´, and d´). The type B embryos of Fig. 4 show asymmetric and scarce TB outgrowth and an ICM with few scattered (Fig. 4eb´), absent (Fig. 4ec´), or disaggregated (Fig. 4ed´) cells.

Figure 4f clearly shows that both the percentage of embryos with type B TB per female and the percentage of embryos with type B ICM per female were significantly lower in treated vs control groups ($p = 0.0025$ and $p = 0.0002$, respectively). On the other hand, we did not observe differences in the number of pups per litter (Fig. 4g) or in their sex distribution (Fig. 4h).

After 7 days of culture, embryos from the treated group but not from the control group presented positive annexin V-FITC marks (Fig. 5). Annexin V-FITC labeled embryos from the treated group showed an intense green fluorescence in the ICM and a light fluorescence in the TB (Fig. 5e and f), whereas only DAPI labeling was observed in the nuclei of embryos from the control group (Fig. 5d). The median fluorescence intensity was significantly higher both in treated TB than in control TB ($p = 0.0028$) and in treated ICM than in control ICM ($p = 0.0007$).

Analysis of the integrity of the sperm and the germ line from male offspring

No significant differences were observed in F-1 sperm viability between both experimental groups (57.6 ± 0.5 in control mice vs. 56.6 ± 1.9 in treated mice, mean ± SEM, Student's *t* test, $p > 0.05$, $n = 5$ males per group). Similarly, upon analysis of the level of oxidative stress, both

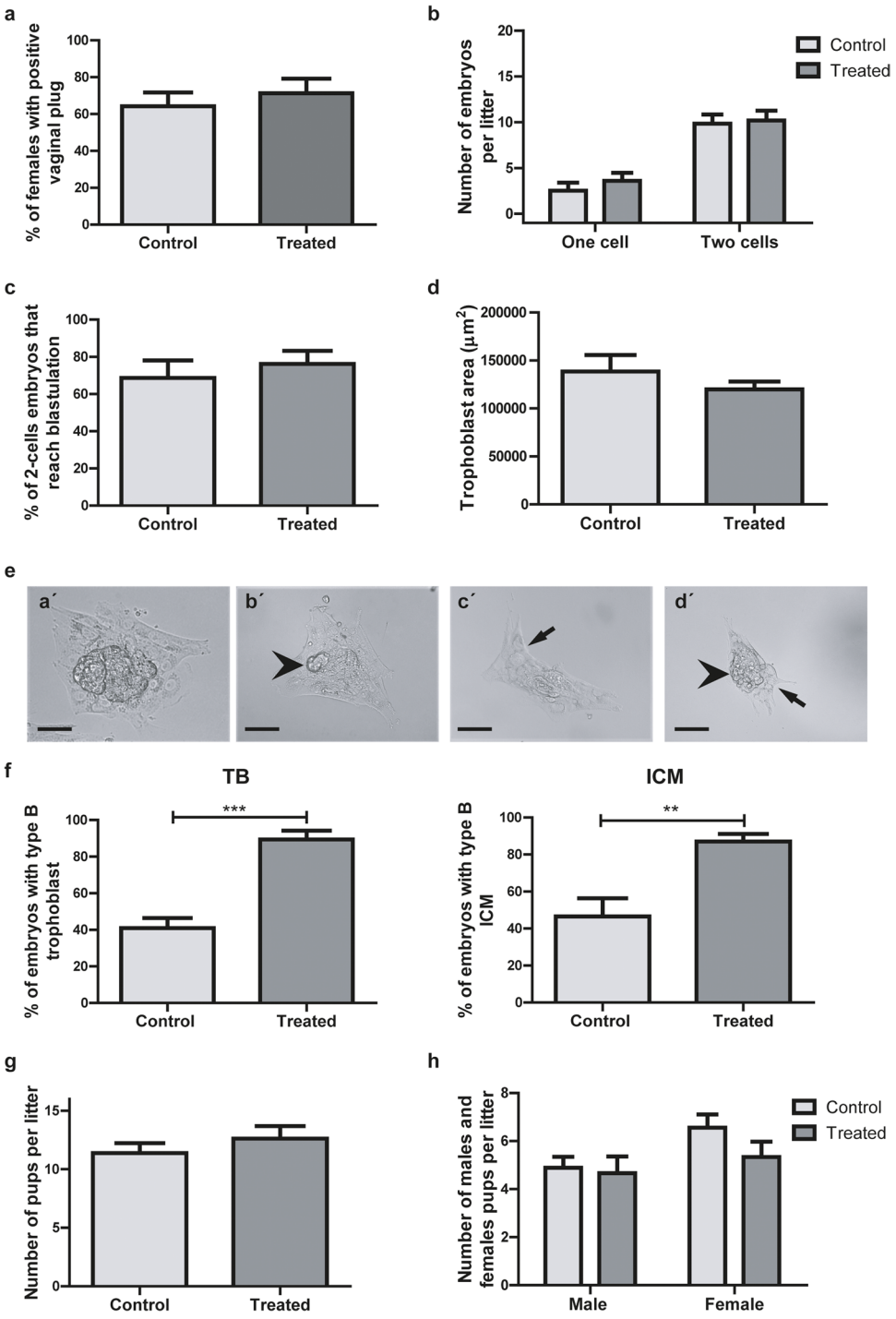

Fig. 4 Embryonic development. **a** Positive vaginal plug proportion ($n=11$ males per group). **b** Number of one or two-cell embryos. ($n=11$ males per group, 4–12 embryos from each). **c** Percentage of two cell embryos that reached the blastocyst stage ($n=9$ males per group, 4–12 embryos from each). **d** Median of outgrowing trophoblast (TB) area per female ($n=11$ males per group, 4–12 embryos from each). **e** Representative images of outgrowing embryos with type A (a´) or B (b´-d´) inner cell mass (ICM)/TB. Arrows indicate asymmetric and scarce trophoblast outgrowth, and arrow heads indicate an ICM with few scattered (b´), absent (c´) or disaggregated (d´) cells. Scale bar, 100 µm. **f** Proportion of embryos with type B TB and ICM morphologies (control, $n=4$ males; treated, $n=6$ males, 4–12 embryos from each). Number of pups (g) and males and females (h) per litter, all in control and treated groups. Data were analyzed by unpaired *t* test ($n=6$ litter per group). Original magnification of images: 400×. $^{**}p<0.01$, $^{***}p<0.001$

the percentage of spermatozoa with a positive mark for the fluorogenic reporter probes used and the relative fluorescence intensity were similar in F1 control and F1 treated groups (Fig. 6a–d).

To assess whether the increase in TUNEL-positive germ cells observed in treated mice was also observed in their male offspring, we analyzed the incidence of nuclear DNA strand breaks in the testes of their progeny. The percentage of spermatozoa with a positive mark for the fluorogenic probes used was similar in both F1 treated and F1 control groups (Fig. 6e and f).

Our group previously showed that the percentage of decondensed spermatozoa was significantly increased in sperm from treated mice following 15 days of 15% (v/v) alcohol consumption, [17]. In this study, we used the same assay to measure sperm decondensation in the offspring (F1)

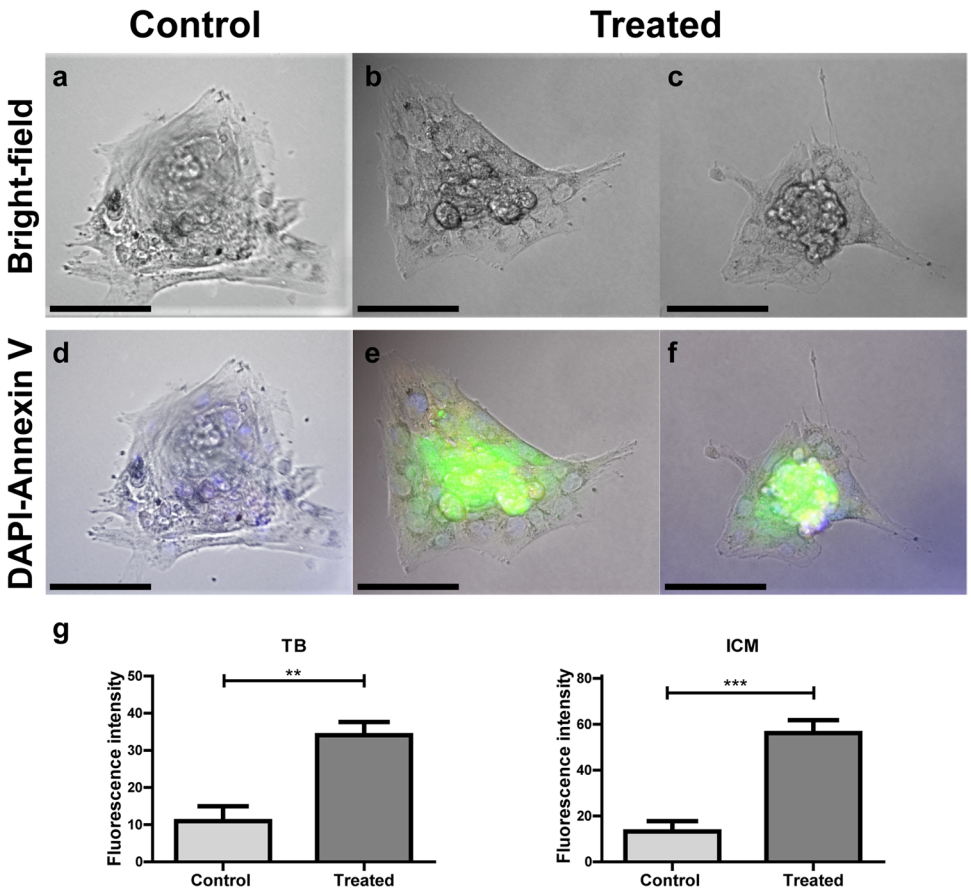

Fig. 5 Cell death detection in two-cell embryos from control or treated groups cultured for 7 days. Embryos were labeled with annexin V-FITC (green) and DAPI (blue) and observed under an epifluorescence inverted microscope (Nikon Eclipse Ti-E). Bright field (**a**, **b**, and **c**) and fluorescence (**d**, **e**, and **f**) microscopic images. Scale bar, 100 µm. Trophoblast (TB) and inner cell mass (ICM) fluorescence intensities (**g**) are presented for control and treated groups. Original magnification 400×, $n = 3$ males per group, 1–2 embryos from each

of mice treated in the same way and did not observe any differences between the F1-treated and F1-control groups. The percentage of decondensed sperm heads was the same in F1-control and F1-treated spermatozoa at all times tested (Fig. 6g).

Testis weight and histological analysis of male offspring

To further evaluate the effects of male mice alcohol consumption on their offspring, we analyzed testicular weight and histology of the progeny. We found that testis weight, both absolute and relative to body weight, was significantly lower in animals of the F1-treated group than in those of the F1-control group ($p = 0.012$ and $p = 0.008$, for absolute and relative weight, respectively) (Table 2). Histological appearances of cross-sections of testes of F1 control and F1 treated mice showed normal seminiferous tubule morphology (20 × magnification). However, at 100 × magnification, irregular spaces were observed in the epithelium, probably due to the desquamation of spermatogenic cells (Fig. 7a). Tubular organization in the testes of F1-treated group males was not altered with respect to F1-control group males, but the diameter of the seminiferous tubules was reduced ($p = 0.0061$) (Fig. 7b). This decrease in seminiferous tubule diameter in the F1-treated group could be attributed to a reduction in the thickness of the seminiferous tubule epithelium ($p = 0.012$) (Fig. 7d), since the size of the lumen of the seminiferous tubules remained unaltered by the treatment (Fig. 7c). When sperm production in the offspring was analyzed, a statistically significant decrease in the efficiency of DSP (DSP per gram of testis) ($p = 0.0152$) was found in F1 treated animals with respect to F1 controls, and a similar, though not significant trend could be observed in the DSP ($p > 0.05$) (Fig. 7f and e, respectively).

Immunofluorescence analysis of PTM of histones in spermatozoa from male offspring

Mouse spermatozoa from male offspring were positive for all histone modifications studied (H3K4me3, H3K27me3, H3K9me2/me3, H3K4me2, H3K9me, H4K12ac). Male alcohol consumption in the parental line significantly increased the abundance of epigenetic histone marks H3K9me ($p = 0.04$) and H4K12ac ($p = 0.04$) in the

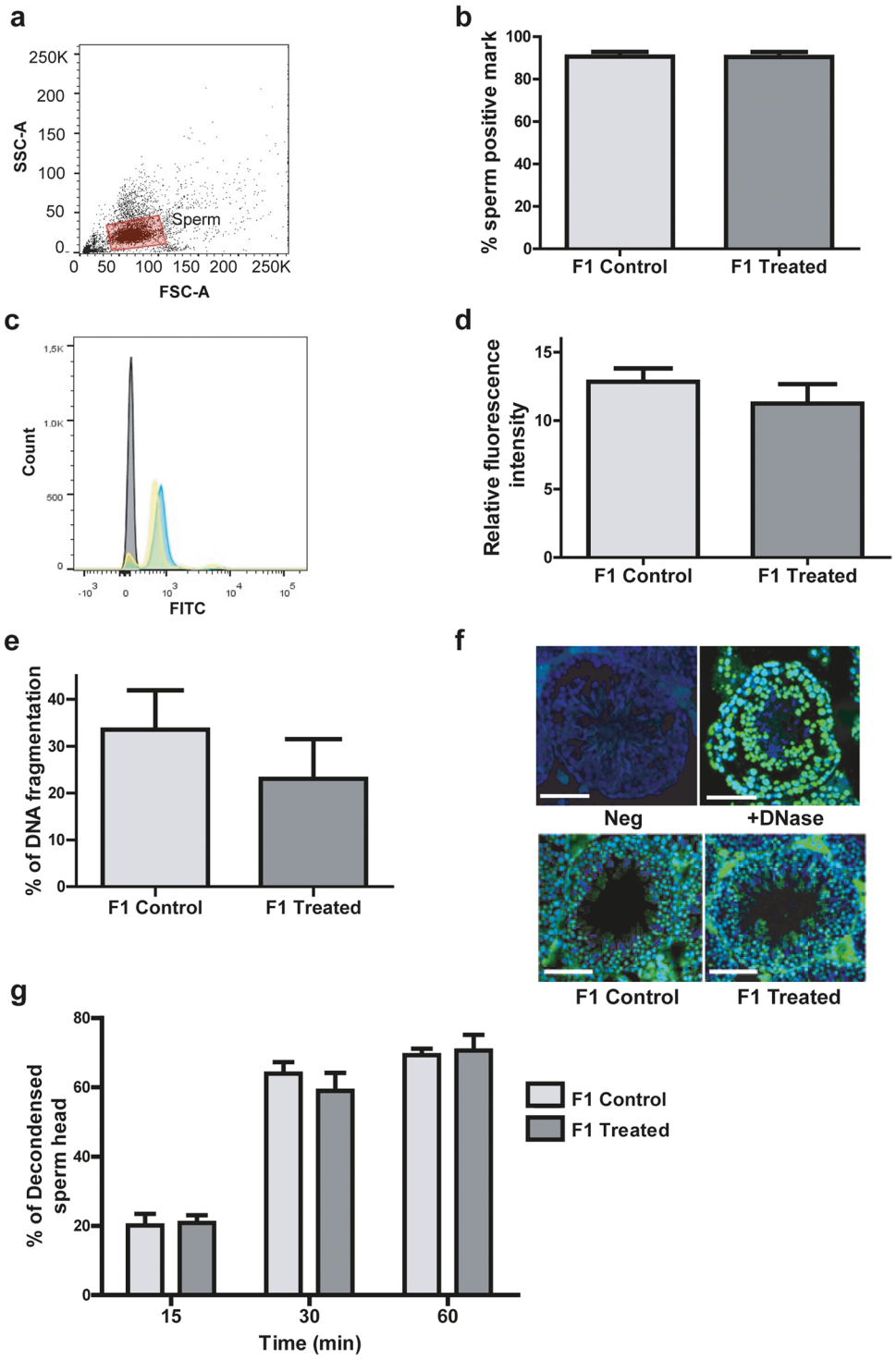

Fig. 6 Analysis of ROS in sperm samples in the progeny (F1). **a** FSC and SSC fluorescence data were collected from 10,000 events per sample. Threshold levels for FSC-A and SSC-A were set to exclude signals from cellular debris or abnormal morphology for all samples. **b** Percentage of spermatozoa evidencing the presence of ROS. **c** Representative histogram of the fluorescence spectra obtained through flow cytometry for sperm samples in absence of reporter probe (grey) and sperm samples corresponding to control (yellow) or treated (blue) mice. **d** Sperm relative fluorescence intensity (positive mark for ROS relative to negative control sample). (**b**, **d**) $p > 0.05$, Nested *t* test, $n = 4$ litter per group (3/4 males in each litter). **e** TUNEL assay results expressed as percentage of DNA fragmentation, $n = 4$ litter per group (3/4 males in each litter) with a minimum of 4 randomly selected fields per testis. Nested *t* test. $p > 0.05$. **f** Representative merge on immunofluorescence images of the TUNEL assay (green: positive TUNEL; blue: DAPI). Scale bar, 100 µm. **g** Mean percentage of decondensed spermatozoa heads at three analyzed times (15, 30, and 60 min). $n = 3$ litter per group (3 males per litter). Data was analyzed with Nested *t* test. $p > 0.05$

spermatozoa of the offspring (Fig. 8e and f, respectively), but no differences were found between experimental groups in the following epigenetic marks: H3K4me3, H3K27me3, H3K9me2/me3, and H3K4me2 (Fig. 8a–d). The localization pattern of modified histones in the sperm head was overall homogenous in all samples analyzed, as had been observed when histone PTMs were analyzed in parent spermatozoa (Fig. 3g).

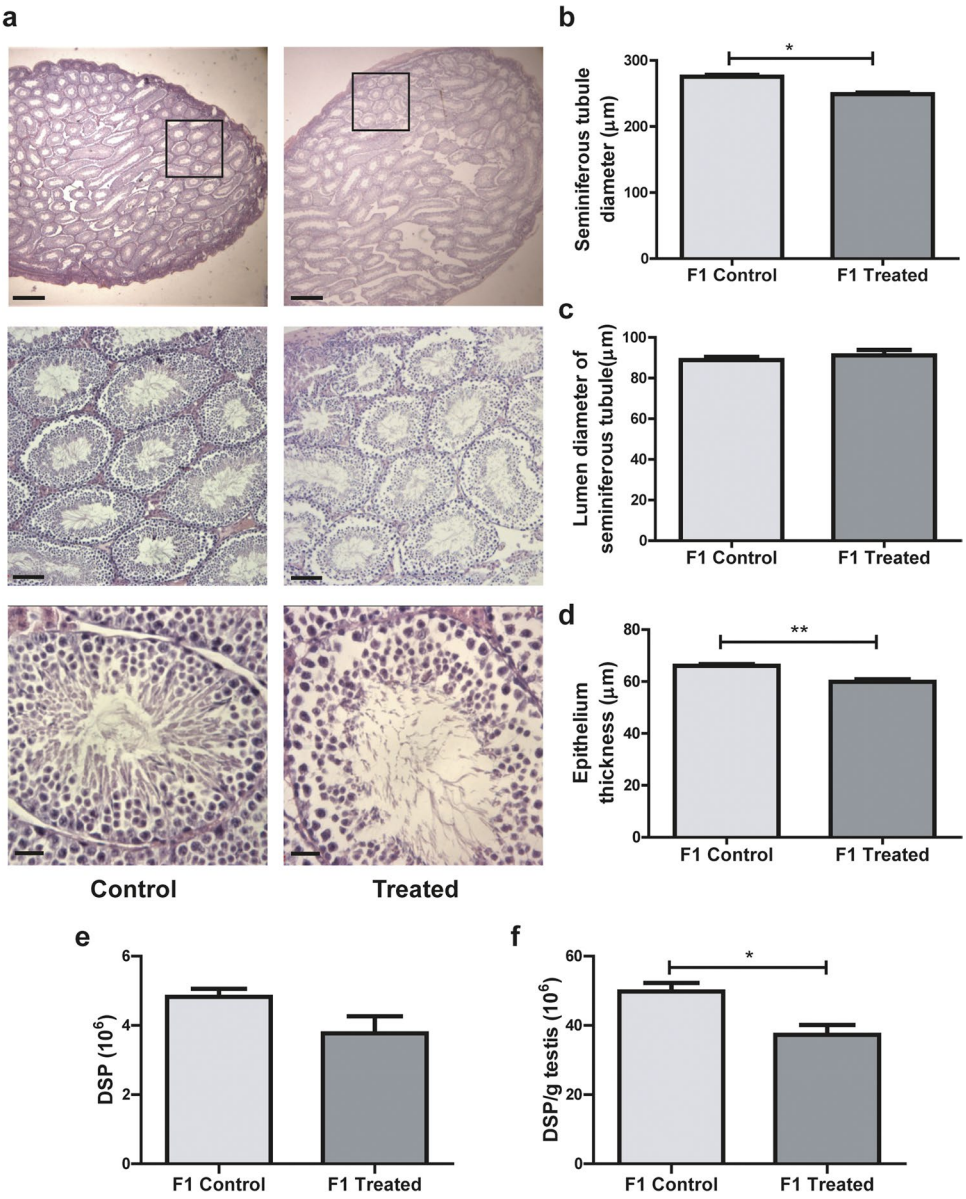

Fig. 7 Testicular histology in the progeny (F1). **a** Cross-section images representative of testicular morphology in control (left panel) and treated (right panel) groups. Stained with Hematoxylin and Eosin. Original magnification of images: 20 × up, 100 × middle, 400 × down (scale bar: 500 µm, 100 µm, and 25 µm, respectively). **b**–**d**) Morphometric analysis of the testes: diameters of seminiferous tubules (**b**), their lumens (**c**), and the thickness of the seminiferous tubule epithelium (**d**). At least 50 tubules were evaluated for each male, $n = 3$ litter per group (3/4 males for each) Nested *t* test. $^*p < 0.05$, $^{**}p < 0.01$. **e** Daily sperm production per testis (DSP) and **f** efficiency (DSP per gram of testis) of sperm production in control and treated group, $n = 5$ litter per group (2/3 males for each). Nested *t* test. $^*p < 0.05$

Discussion

In this study, we explored the impact of paternal alcohol consumption on sperm function, early embryo development, and some aspects of the reproductive health of male offspring.

There was no difference in sperm count between ethanol and control groups in this study, and unlike other reports in which decreased sperm motility is usually described for alcohol-treated animals [26], we found no differences between both groups in this parameter either. Notwithstanding, in a previous work [17], we observed that the percentage of sperm presenting hyperactivated motility was significantly decreased in males treated for a longer period (15 days).

It is well known that sublethal levels of oxidative stress can have a negative impact on the integrity of spermatic DNA, thereby hindering embryo development and having a detrimental effect on progeny health [27–29], and some authors have stated that alcohol consumption increases oxidative stress in spermatozoa [30, 31]. Furthermore, we have previously reported [17] a significant increase in the percentage of decondensed sperm heads in alcohol-treated males, which could render the nuclei of these spermatozoa more susceptible to damage. Accordingly, in this study, we analyzed the levels of ROS in spermatozoa from control and treated male mice and found an increased intensity of ROS markers in spermatozoa of treated animals. Moreover, significantly higher levels of DNA fragmentation in the germ cell line were found in testis cross-sections of the treated

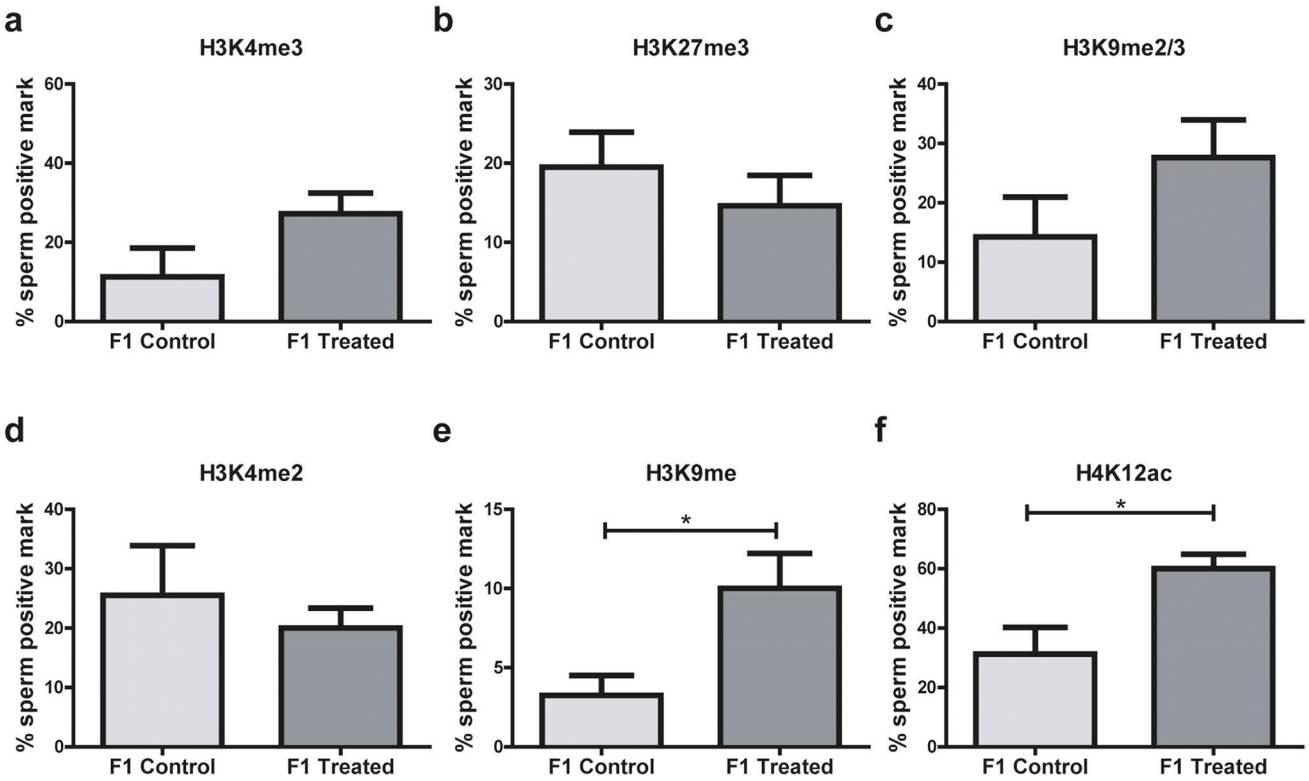

Fig. 8 Post-translational modifications (PTM) of histones in spermatozoa from the progeny. **a** H3K4me3, **b** H3K27me3, **c** H3K9me2/3, **d** H3K4me2, **e** H3K9me, **f** H4K12ac, $n = 4$ litter per group (3 males per litter). Data were analyzed with Student's t test for parametric data or Mann–Whitney U tests for non-parametric data, $^{*}p < 0.05$

group, probably affecting the formation of healthy mature spermatozoa. Taken together, these results indicate that alcohol consumption could be affecting the integrity of the germline within the testis through an increase in ROS, which could in turn be damaging sperm chromatin. This could in turn cause defects in proper gamete formation, including heritable epigenetic modifications which could have adverse effects on the offspring. We also found histopathological alterations in testicular sections of treated animals, both in the seminiferous tubules and the interstitial space. Morphometric analysis revealed an increase in the diameter of the lumen of the seminiferous tubules of treated mice, while there were no differences in either tubule diameter or epithelium thickness between control and treated groups, suggesting that alcohol consumption under our experimental conditions could alter the morphology of the male gonad. Previous studies have reported that variations in lumen diameter could be attributed to an ethanol induced increase in ROS, which eventually results in structural damage [32, 33]. There is also evidence in the literature that substance consumption has a toxic effect on spermatogenesis, affecting division of spermatogonia, increasing germ cell degeneration and phagocytosis, delaying spermatogenesis, and increasing germ cell sloughing [34, 35].

Interestingly, these histological alterations did not correlate with sperm concentration, which was similar in both experimental groups. This inconsistency could be attributed to the fact that sperm count was determined in our previous study using spermatozoa collected from the epididymal *cauda* and is thus indicative of sperm accumulation in this region of the epididymis, probably not allowing to correctly assess alterations in sperm production caused by alcohol intoxication during the experimental treatment. In fact, when we analyzed DSP, we observed a decrease in the number of spermatids per testis in the ethanol treated group, indicating that alcohol consumption is detrimental to sperm production, as was previously reported in a study in which alcohol intake was negatively associated with sperm count [36].

It is known that chronic alcohol exposure in male mice affects gene methylation in their spermatozoa and that these alterations which are then transmitted to their offspring, generate mental disorders [15]. Even alcohol concentrations that do not inhibit embryonic growth can produce genetic or chromosomal abnormalities in gametes. Notably, Knezovich and Ramsay have shown that alcohol-induced epigenetic changes could be responsible for transgenerational effects in mice [14]. In this study, we analyzed six histone PTMs to assess whether alcohol

consumption altered their proportion in mature spermatozoa. These PTMs were selected due to their association with genes expressed early in embryonic development [37–41]. All marks were observed in the sperm head, and some also appeared in the midpiece; this staining observed in the midpiece is by no means nonspecific. Immunofluorescence analysis revealed the presence of modified histones H3K27me3 and H4ac in sperm tails, which was further corroborated by Western blotting, thus confirming that those marks did not correspond to a nonspecific binding. This analysis clearly demonstrated that the proteins extracted from sperm tails included residual histones with specific PTMs. Similar marks were found when analyzing human sperm cells (data not shown), in agreement with Krejci et al. (2015) who previously reported the presence of remanent histones in the tail of human spermatozoa [42]. There is no evidence in the scientific literature of a similar study in mice, but we strongly believe that our findings clearly indicate the presence of histones in the tails of sperm cells. Our results showed reduced levels of H3K4me3, suggesting that ethanol could be altering this PTM. Bernstein et al. [43] reported the presence of H3K4me3 in the coding regions of active genes and in human sperm; the H3K4me3 mark is localized in paternally expressed imprinted loci and promoters of developmental genes, thus suggesting that this paternal mark plays a key role in the developmental programs of the embryo [44].

Information in the literature indicates that the retention of the H3K4me3 mark in spermatozoa is most likely crucial during fertilization and early embryo development and that its reduction due to alcohol consumption as shown in this study could negatively affect both processes.

Not all histones are replaced by protamines during spermiogenesis, denoting that nucleosome retention in certain regions of the DNA is probably relevant to fertilization and embryonic development. Hammoud et al. described that DNA associated with the retained nucleosomes is abundant in microRNA promoters, imprinted genes, and genes essential to early mammalian development, such as HOX genes [13].

We then evaluated the success of in vivo fertilization and in vitro early embryonic development in our experimental model. We did not detect differences in the appearance of the vaginal plug 24 h after mating, nor in the number of one or two-cell embryos obtained after female dissection, an additional 24 h post-positive vaginal plug. These observations are consistent with our previous finding that sperm from mice under a similar intoxication scheme (15-day treatment), which showed increased nuclear decondensation, were successful at fertilizing oocytes from control females during in vitro fertilization [17]. Thus, spermatozoa from treated males do not have an impairment to reach the fertilization site or fertilize the oocyte.

Considering that activation of the paternal genome takes place in mice in the pre-implantation embryo [45], we cultured two-cell embryos for 7 days and observed morphological changes in the development of the ICM and TB of embryos from the treated group but found no differences in their TB outgrowth areas.

We did detect the presence of possible apoptotic marks in embryos of the treated group at this same stage of development, an observation which needs further investigation. For many years, embryonic morphology has been used as an indicator of viability and correlates with the ability of embryos to implant in the maternal uterus.

Many researchers have used embryo morphology as a quality parameter, not only as a tool for research but also in the assisted reproduction clinic to transfer embryos with a greater potential to successfully implant [46, 47]. The present study provides a detailed description of the changes found in developing embryos, where the observation of outgrowths allows us to classify the ICM and TB into type A or B, as previously reported [23]. Considering that the ability of peri-implantation blastocysts to produce an outgrowth reflects their potential for in utero implantation [24], we expected to find that in vivo, paternal alcohol consumption would affect the birth of the progeny. However, this did not happen in our model. We hypothesize that the sublethal effect of parental alcohol consumption on developing embryos is more evident in an in vitro culture system, where the developing embryo is missing all interaction with the uterine microenvironment which could certainly compensate certain embryo deficiencies.

Few authors have studied the effect of alcohol consumption on early embryonic development and have usually done so under a model of female consumption. Some of these studies have described comparable alterations when a similar alcohol content (12.5% v/v) was administered to female rats 4 days pre- and post-conception [48], showing effects on TB differentiation, as well as on placental function at day 15 of gestation. Likewise, Pérez-Tito et al. reported that a 10% v/v alcohol intoxication scheme in CF-1 female mice, for 14 days prior to and 4/5 days following conception, caused alterations in embryonic development and TB outgrowth [49].

Another study evaluated the effects of a moderate episodic exposure model in female rats to mimic "special occasion" drinking (ethanol gavage, 1 g ethanol/kg body weight), which did not impact on the fertility of their female offspring [50]. However, we could not find any studies describing effects of paternal alcohol intake on early embryonic development, but some authors have indeed concluded that paternal alcohol consumption significantly affects the offspring. Particularly, Chang et al.

reported that chronic pre-conceptional ethanol exposure in male mice (10% w⁄v ethanol, 4 h a day for 70 days) associates with fetal growth restriction, decreased placental efficiency, abnormalities in cholesterol trafficking, sex-specific alterations in the genetic pathways regulating hepatic fibrosis, and disruptions in the regulation of imprinted genes at day 14.5 of gestation [51]. Similarly, other authors [52] showed that under the same intoxication scheme, there is an association between chronic preconceptional paternal alcohol consumption and deficits in offspring growth, concluding that alcohol exposure did not alter male reproductive physiology or fertility but did induce late-term fetal growth restriction in the offspring at gestational day 16.5. This result correlated with alterations in sperm-inherited non-coding RNAs. Furthermore, Chang et al. reported that, under the same intoxication scheme, male offspring presented metabolic defects associated with dysregulation of genes in the liver and pancreas [53].

Even more so, paternal alcohol exposure has also been shown to alter the function of the hypothalamic–pituitary–adrenal axis in the offspring of alcohol treated rats [54], and there is a reported relationship between paternal stress and alcohol consumption, which act similarly to influence the alcohol-drinking and stress phenotypes of the next generation [55]. In our lab, we have observed significant changes in morphometric characteristics, in behavior and in immune populations in the progeny of alcoholic males (not published), which leads us to believe that it is essential to continue with the study of the progeny, particularly with embryonic development.

We continued with the evaluation of the effect of paternal alcohol consumption on the reproductive health of their adult male offspring. No changes were observed in either ROS levels in sperm or DNA fragmentation in the germline of the offspring of F1-treated animals, suggesting that only direct alcohol consumption increases ROS levels, causing DNA fragmentation in the germ cell line and nuclei damage in the resulting sperm cells. Additionally, and contrary to what we reported previously for the parental line following a 15-day alcohol consumption [17], there were no differences in sperm nuclear decondensation in the progeny of F1-control and F1-treated groups.

Although no major alterations were observed at the histopathological level in the testes of mice in the F1-treated group, there was a reduction in testicular weight in its progeny. This correlated with the decrease in the diameter of the seminiferous tubules and the decrease of epithelium thickness of the tubule wall, where the sperm germline is located. In addition, although we did not find differences in sperm count between F1-control and F1-treated groups, we did find a smaller number of spermatids per testis weight in F1-treated animals, suggesting that paternal alcohol consumption could alter the offspring's spermatozoa production.

Regarding PTMs in spermatozoa of the progeny, we found increased H3K9me and H4K12ac marks in the F1-treated group, suggesting a transgenerational effect of paternal alcohol consumption on sperm chromatin epigenetic modifications. Van der Heijden et al. reported that sperm rapidly decondense after fertilization and that their chromatin is associated with oocyte histones, but it retain the spermatic H4K12ac marks [56]. Brykczynska et al. proposed that environmental factors and behavioral habits can generate variability and retention of modified histones in sperm and cause incomplete chromatin remodeling during sperm development [38]. Even though we did not observe an increase in this mark in the parental line, alcohol consumption could be favoring either the retention of this modified histone in the sperm of male offspring through some yet to be discovered mechanism or its de novo incorporation in the progeny. It is well known that alteration of histone PTMs in spermatozoa are relevant to sperm cell physiology. Histone H3K9 modification increases during meiosis in spermatogenesis but must be removed by the end of spermiogenesis [57–59]. This PTM has also been associated to Prm1 y Tnp1 promoters, as a repressor of these two genes whose expression is crucial for an adequate spermiogenesis.

Gaydos et al. have reported that the presence of H3K9 is a repressive mark via the heterochromatin formation in *C. elegans* sperm and show that H3K9 methylation provides an alternative way to transmit X repression to the progeny, probably through retention of the heterochromatic status acquired during spermatogenesis [60]. On the other hand, H4K12ac, which is passed on to the zygote, has been associated with paternal influence on gene expression in the zygote and could be involved in early embryo development [56]. This PTM has been found in the vicinity of transcription initiation sites of genes heavily expressed in early zygotes and genes associated with chromatin organization [61], and the authors have suggested that aberrant histone acetylation sperm could reflect anomalies in chromatin compaction that might result in inadequate transfer of epigenetic information to the oocyte. Vieweg et al. have reported that H4K12ac colocalizes with 5mC in the sperm nucleus and that it could play an important role in the harvesting of transcription factors and regulation of gene expression during early embryogenesis [62].

Several authors have analyzed the impact of maternal alcohol consumption on the offspring, but the effect of paternal alcohol consumption has been poorly investigated. Further studies that focus on paternal consumption are needed to shift towards a paradigm that acknowledges the decisive paternal contribution to the deleterious transgenerational effects of alcohol intoxication, rather than considering maternal consumption as their only cause. This study provides relevant contributions on the direct effect of ethanol intake on the germline of intoxicated males

and on some of its indirect effects on the reproductive health of the male progeny. The evidence presented in this paper regarding the intergenerational effects of paternal alcohol exposure stresses the need to further this study. We consider it particularly relevant to evaluate the presence of histone modifications at different stages of early embryonic development and to assess the reproductive potential of male offspring of alcohol treated males, to identify possible consequences that epigenetic modifications might have on their fecundity or their progeny (F2). If a correlation between PTM modifications and damage in the progeny were to be confirmed, it could have important implications in the clinical setting because histone PTMs could be investigated in human spermatozoa prior to their use in an assisted reproduction procedure. We believe that it is of the utmost importance that we continue this study.

Acknowledgements The authors wish to acknowledge Dr. Lucrecia Piñeiro for helping us with statistical interpretation of the data and technician Zaira Naguila for her collaboration and support in handling animals, as well as all the staff of the Central Bioterio of the University of Buenos Aires.

Author contribution MYC performed experiments, analyzed data, and wrote the paper. LG performed experiments and analyzed data. MGS was involved in animal care and treatment and language correction. SB involved in animal care and treatment. GS performed cell death experiments. MR analyzed data and corrected the paper. JCC supervised the study and corrected the paper. VAF conceived the study and wrote the paper.

Funding This work was supported by a grant from Fundación Honorio Bigand, Buenos Aires, Argentina. MYC and LG are doctoral fellows, CONICET, Argentina.

Declarations

Ethics approval This study was approved by the CICUAL (Comisión Institucional de Cuidado y Uso de Animales de Laboratorio) of FCEN-UBA (Protocol Number 56/2016).

Conflict of interest The authors declare no competing interests.

References

1. Dimijian GG. Evolution of sexuality: biology and behavior. Proc (Bayl Univ Med Cent). 2005;18(3):244–58.
2. Stearns SC. The evolutionary maintenance of sexual reproduction: the solutions proposed for a longstanding problem. J Genet. 1990;69(1):1–10.
3. Otto S. Sexual Reproduction and the Evolution of Sex. Nature Education. 2008;1:182.
4. Marchiani S, Tamburrino L, Benini F, et al. Chromatin protamination and catsper expression in spermatozoa predict clinical outcomes after assisted reproduction programs. Sci Rep. 2017;7(1):15122. https://doi.org/10.1038/s41598-017-15351-3.
5. Meyer RG, Ketchum CC, Meyer-Ficca ML. Heritable sperm chromatin epigenetics: a break to remember. Biol Reprod. 2017;97(6):784–97. https://doi.org/10.1093/biolre/iox137.
6. Sakkas D, Alvarez JG. Sperm DNA fragmentation: mechanisms of origin, impact on reproductive outcome, and analysis. Fertil Steril. 2010;93(4):1027–36. https://doi.org/10.1016/j.fertnstert.2009.10.046.
7. Henkel RR, Franken DR. Sperm DNA fragmentation: origin and impact on human reproduction. J Reprod Stem Cell Biotechnol. 2011;2(2):88–108. https://doi.org/10.1177/205891581100200204.
8. Asmarinah, Syauqy A, Umar LA, et al. Sperm chromatin maturity and integrity correlated to zygote development in ICSI program. Syst Biol Reprod Med. 2016;62(5):309–316. https://doi.org/10.1080/19396368.2016.1210695
9. Donkin I, Barrès R. Sperm epigenetics and influence of environmental factors. Mol Metab. 2018;14:1–11. https://doi.org/10.1016/j.molmet.2018.02.006.
10. Giacone F, Cannarella R, Mongioì LM, et al. Epigenetics of male fertility: effects on assisted reproductive techniques. World J Mens Health. 2019;37(2):148–56. https://doi.org/10.5534/wjmh.180071.
11. Nanassy L, Carrell DT. Paternal effects on early embryogenesis. J Exp Clin Assist Reprod. 2008;5:2. https://doi.org/10.1186/1743-1050-5-2.
12. Teperek M, Simeone A, Gaggioli V, et al. Sperm is epigenetically programmed to regulate gene transcription in embryos. Genome Res. 2016;26(8):1034–46. https://doi.org/10.1101/gr.201541.115.
13. Hammoud SS, Purwar J, Pflueger C, et al. Alterations in sperm DNA methylation patterns at imprinted loci in two classes of infertility. Fertil Steril. 2010;94(5):1728–33. https://doi.org/10.1016/j.fertnstert.2009.09.010.
14. Knezovich JG, Ramsay M. The effect of preconception paternal alcohol exposure on epigenetic remodeling of the h19 and rasgrf1 imprinting control regions in mouse offspring. Front Genet. 2012;3:10. https://doi.org/10.3389/fgene.2012.00010.
15. Liang F, Diao L, Liu J, et al. Paternal ethanol exposure and behavioral abnormities in offspring: associated alterations in imprinted gene methylation. Neuropharmacology. 2014;81:126–33. https://doi.org/10.1016/j.neuropharm.2014.01.025.
16. Sánchez MC, Alvarez Sedó C, Chaufan GR, et al. In vitro effects of endosulfan-based insecticides on mammalian sperm. Toxicol Res (Camb). 2017;7(1):117–26. https://doi.org/10.1039/c7tx00251c.
17. Sánchez MC, Fontana VA, Galotto C, et al. Murine sperm capacitation, oocyte penetration and decondensation following moderate alcohol intake. Reproduction. 2018;155(6):529–41. https://doi.org/10.1530/REP-17-0507.
18. Zindy F, den Besten W, Chen B, et al. Control of spermatogenesis in mice by the cyclin D-dependent kinase inhibitors p18(Ink4c) and p19(Ink4d). Mol Cell Biol. 2001;21(9):3244–55. https://doi.org/10.1128/MCB.21.9.3244-3255.2001.
19. Fraser LR, Drury LM. The relationship between sperm concentration and fertilization in vitro of mouse eggs. Biol Reprod. 1975;13(5):513–8. https://doi.org/10.1095/biolreprod13.5.513.
20. Kyjovska ZO, Boisen AMZ, Jackson P, et al. Daily sperm production: application in studies of prenatal exposure to nanoparticles in mice. Reprod Toxicol. 2013;36:88–97. https://doi.org/10.1016/j.reprotox.2012.12.005.
21. Nanjappa MK, Hess RA, Medrano TI, et al. Membrane-localized estrogen receptor 1 is required for normal male reproductive development and function in mice. Endocrinology. 2016;157(7):2909–19. https://doi.org/10.1210/en.2016-1085.
22. Sanchez MC, Sedo CA, Julianelli VL, et al. Dermatan sulfate synergizes with heparin in murine sperm chromatin decondensation. Syst Biol Reprod Med. 2013;59(2):82–90. https://doi.org/10.3109/19396368.2012.756952.

23. Fontana V, Choren V, Vauthay L, et al. Exogenous interferon-gamma alters murine inner cell mass and trophoblast development. Effect on the expression of ErbB1, ErbB4 and heparan sulfate proteoglycan (perlecan). Reproduction. 2004;128(6):717–25. https://doi.org/10.1530/rep.1.00335F.
24. Enders AC, Chávez DJ Schlafke S. Comparison of implantation in utero and in vitro. In: Glasser S.R., Bullock D.W, editors. Cellular and molecular aspects of implantation. Springer, Boston, MA; 1981. https://doi.org/10.1007/978-1-4613-3180-3_29
25. Salamone G, Giordano M, Trevani AS, et al. Promotion of neutrophil apoptosis by TNF-alpha. J Immunol. 2001;166(5):3476–83. https://doi.org/10.4049/jimmunol.166.5.3476.
26. Condorelli RA, Calogero AE, Vicari E, et al. Chronic consumption of alcohol and sperm parameters: our experience and the main evidences. Andrologia. 2015;47(4):368–79. https://doi.org/10.1111/and.12284.
27. Aitken RJ, Gordon E, Harkiss D, et al. Relative impact of oxidative stress on the functional competence and genomic integrity of human spermatozoa. Biol Reprod. 1998;59(5):1037–46. https://doi.org/10.1095/biolreprod59.5.1037.
28. Aitken RJ, Curry BJ. Redox regulation of human sperm function: from the physiological control of sperm capacitation to the etiology of infertility and DNA damage in the germ line. Antioxid Redox Signal. 2011;14(3):367–81. https://doi.org/10.1089/ars.2010.3186.
29. Aitken RJ. Not every sperm is sacred; a perspective on male infertility. Mol Hum Reprod. 2018;24(6):287–98. https://doi.org/10.1093/molehr/gay010.
30. Harikrishnan R, Abhilash PA, Syam Das S, et al. Protective effect ascorbic acid against ethanol-induced reproductive toxicity in male guinea pigs. Br J Nutr. 2013;110(4):689–98. https://doi.org/10.1017/S0007114512005739.
31. Maneesh M, Dutta S, Chakrabarti A, et al. Alcohol abuse-duration dependent decrease in plasma testosterone and antioxidants in males. Indian J Physiol Pharmacol. 2006;50(3):291–6.
32. Kuladip J, Prabhat KS, Dipak KD. Nicotine diminishes testicular gametogenesis, steroidogenesis, and steroidogenic acute regulatory protein expression in adult albino rats: possible influence on pituitary gonadotropins and alteration of testicular antioxidant status. Toxicol Sci. 2010;116(2):647–59. https://doi.org/10.1093/toxsci/kfq149.
33. Jalili C, Salahshoor MR, Naseri A. Protective effect of Urtica dioica L against nicotine-induced damage on sperm parameters, testosterone and testis tissue in mice. Iran J Reprod Med. 2014;12(6):401–8.
34. Russell LD, Sinhá- Hikim AP, Ettlin RA, et al. Evaluation of the testis: histological and histopathological. 1ed. Cache River Press, 1990.
35. Rocha NR, Braz JKFDS, de Souza SRG, et al. Testicular morphometry of rats with Walker 256 tumor supplemented with L-glutamine. Anim Reprod. 2021;18(2):e20200051 https://doi.org/10.1590/1984-3143-AR2020-0051
36. Veron GL, Tissera AD, Bello R, et al. Impact of age, clinical conditions, and lifestyle on routine semen parameters and sperm kinematics. Fertility & Sterility 2018;110 68–75.e4 https://doi.org/10.1016/j.fertnstert.2018.03.016.
37. Shi L, Wu J. Epigenetic regulation in mammalian preimplantation embryo development. Reprod Biol Endocrinol. 2009;7:59. Published 2009 Jun 5. https://doi.org/10.1186/1477-7827-7-59
38. Brykczynska U, Hisano M, Erkek S, et al. Repressive and active histone methylation mark distinct promoters in human and mouse spermatozoa. Nat Struct Mol Biol. 2010;17(6):679–87. https://doi.org/10.1038/nsmb.1821.
39. Carrell DT, Hammoud SS. The human sperm epigenome and its potential role in embryonic development. Mol Hum Reprod. 2010;16(1):37–47. https://doi.org/10.1093/molehr/gap090.
40. Boissonnas CC, Jouannet P, Jammes H. Epigenetic disorders and male subfertility. Fertil Steril. 2013;99(3):624–31. https://doi.org/10.1016/j.fertnstert.2013.01.124.
41. Jung YH, Sauria MEG, Lyu X, et al. Chromatin states in mouse sperm correlate with embryonic and adult regulatory landscapes. Cell Rep. 2017;18(6):1366–82. https://doi.org/10.1016/j.celrep.2017.01.034.
42. Krejčí J, Stixová L, Pagáčová E, et al. Post-translational modifications of histones in human sperm. J Cell Biochem. 2015;116(10):2195–209. https://doi.org/10.1002/jcb.25170.
43. Bernstein BE, Humphrey EL, Erlich RL, et al. Methylation of histone H3 Lys 4 in coding regions of active genes. Proc Natl Acad Sci U S A. 2002;99(13):8695–700. https://doi.org/10.1073/pnas.082249499.
44 Samson M, Jow MM, Wong CC, et al. The specification and global reprogramming of histone epigenetic marks during gamete formation and early embryo development in C. elegans. PLoS Genet. 2014;10(10):e1004588. https://doi.org/10.1371/journal.pgen.1004588.
45. Latham KE, Schultz RM. Embryonic genome activation. Front Biosci. 2001;6:D748–59. https://doi.org/10.2741/latham.
46. Jansen R, Mortimer D. Gardner's system for grading human blastocysts. Adapted from: Gardner and Schoolcraft, 1999a. In vitro culture of human blastocysts. Toward Reproductive Certainty: Fertility and Genetics Beyond. London: Parthenon. 1999;378–388
47. Machtinger R, Racowsky C. Morphological systems of human embryo assessment and clinical evidence. Reprod Biomed Online. 2013;26(3):210–21. https://doi.org/10.1016/j.rbmo.2012.10.021.
48. Kalisch-Smith JI, Steane SE, Simmons DG, et al. Periconceptional alcohol exposure causes female-specific perturbations to trophoblast differentiation and placental formation in the rat. Development. 2019;146(11):dev172205. https://doi.org/10.1242/dev.172205.
49. Pérez-Tito L, Bevilacqua E, Cebral E. Peri-implantational in vivo and in vitro embryo-trophoblast development after perigestational alcohol exposure in the CD-1 mouse. Drug Chem Toxicol. 2014;37(2):184–97. https://doi.org/10.3109/01480545.2013.834358.
50. McReight EK, Liew SH, Steane SE, et al. Moderate episodic prenatal alcohol does not impact female offspring fertility in rats. Reproduction. 2020;159(5):615–26. https://doi.org/10.1530/REP-20-0039.
51. Chang RC, Skiles WM, Chronister SS, et al. DNA methylation-independent growth restriction and altered development programming in a mouse model of preconception male alcohol exposure. Epigenetics. 2017;12(10):841–53. https://doi.org/10.1080/15592294.2017.1363952.
52. Bedi Y, Chang RC, Gibbs R, et al. Alterations in sperm-inherited noncoding RNAs associate with late-term fetal growth restriction induced by preconception paternal alcohol use. Reprod Toxicol. 2019;87:11–20. https://doi.org/10.1016/j.reprotox.2019.04.006.
53. Chang RC, Wang H, Bedi Y, et al. Preconception paternal alcohol exposure exerts sex-specific effects on offspring growth and long-term metabolic programming. Epigenetics Chromatin. 2019;12(1):9. https://doi.org/10.1186/s13072-019-0254-0.
54. Govorko D, Bekdash RA, Zhang C, et al. Male germline transmits fetal alcohol adverse effect o hypothalamic proopiomelanocortin gene across generations. Biol Psychiatry. 2012;72(5):378–88. https://doi.org/10.1016/j.biopsych.2012.04.006.
55. Rompala GR, Simons A, Kihle B, et al. Paternal preconception chronic variable stress confers attenuated ethanol drinking behavior selectively to male offspring in a pre-stress environment dependent manner. Front Behav Neurosci. 2018;12:257. https://doi.org/10.3389/fnbeh.2018.00257.
56. van der Heijden GW, Derijck AA, Ramos L, et al. Transmission of modified nucleosomes from the mouse male germline to the

zygote and subsequent remodeling of paternal chromatin. Dev Biol. 2006;298(2):458–69. https://doi.org/10.1016/j.ydbio.2006.06.05.
57. Okada Y, Scott G, Ray M, et al. Histone demethylase JHDM2A is critical for Tnp1 and Prm1 transcription and spermatogenesis. Nature. 2007;450:119–23. https://doi.org/10.1038/nature06236.
58. Capra E, Lazzari B, Turri F, et al. Epigenetic analysis of high and low motile sperm populations reveals methylation variation in satellite regions within the pericentromeric position and in genes functionally related to sperm DNA organization and maintenance in Bos taurus. BMC Genomics. 2019;20(1):940. https://doi.org/10.1186/s12864-019-6317-6.
59. Ge S, Zhao P, Liu X, et al. Necessity to evaluate epigenetic quality of the sperm for assisted reproductive technology. Reprod Sci. 2019;26(3):315–22. https://doi.org/10.1177/1933719118808907.
60. Gaydos LJ, Wang W, Strome S. Gene repression. H3K27me and PRC2 transmit a memory of repression across generations and during development. Science. 2014;345(6203):1515–1518. https://doi.org/10.1126/science.1255023
61. Paradowska AS, Miller D, Spiess AN, et al. Genome wide identification of promoter binding sites for H4K12ac in human sperm and its relevance for early embryonic development. Epigenetics. 2012;7(9):1057–70. https://doi.org/10.4161/epi.21556.
62. Vieweg M, Dvorakova-Hortova K, Dudkova B, et al. Methylation analysis of histone H4K12ac-associated promoters in sperm of healthy donors and subfertile patients. Clin Epigenetics. 2015;7(1):31. https://doi.org/10.1186/s13148-015-0058-4.